Universität Regensburg
Mathematik

A phase-field model for multiphase systems with preserved volume fractions

Britta Nestler, Frank Wendler, Michael Selzer,
Harald Garcke and Björn Stinner

Preprint Nr. 01/2008

A phase-field model for multiphase systems with preserved volume fractions

Britta Nestler, Frank Wendler, Michael Selzer
Institute of Computational Engineering, Karlsruhe University of Applied Sciences, Moltkestrasse 30, D–76133 Karlsruhe, Germany

Björn Stinner, Harald Garcke
NWF I - Mathematik, Universität Regensburg, D–93040 Regensburg, Germany
(Dated: January 2, 2008)

We report on a novel formulation of a phase-field model which incorporates a description of individual phases and particles with preserved volume evolving in a system of multiple phases such that the interfacial energy decreases. In our model, an anti-forcing free energy density is defined to fulfill constraints on selected volume fractions by counterbalancing phase changes. Phases are defined as regions with energy bearing boundaries that may differ in their physical states, i.e., the regions may distinguish in structure (crystal transformations), in composition (alloys, mixtures of fluids), or in the orientation of the crystal lattice (grains). The method allows to simulate the formation of equilibrium crystal shapes and of the migration of inert particles and phases in microstructures. We show 2D and 3D simulations of bubble ensembles and foam textures and demonstrate the excellent agreement of crystal morphology configurations with analytical results.

PACS numbers: 81.10.Aj, 47.57.Bc, 47.55.db 05.70.Ln, 61.72.Mm, 61.72.Qq

Inhomogeneous systems characterized by multiple regions of different physical states, which will be called phases in the following, frequently involve energy contributions located along the phase interfaces. In this letter, we consider the evolution of multi-phase systems in which the interfacial energy decreases and some of the phases obey volume constraints, i.e., on the time scale of the interface motion, volume changes of those phases due to more or less complex physical processes can be neglected. Applications of models for such systems range from grain coarsening with inert inclusions [1, 2] over the determination of foam structures [3] and bubble clusters [4] to crystal growth with surface attachment limited kinetics [5] and morphologies of double crystals [6]. A previously developed phase-field model [7] has been generalized in order to take volume constraints into account. Multi-well potentials of obstacle type revealed to be advantageous with respect to the calibration of surface energy densities [8, 9] but lead to variational inequalities and, therefore, require a special numerical treatment as, e.g., in [10]. After deriving the model equations and the numerical treatment, simulation results of bubble ensembles, foam structures and double crystals are presented. We consider a general system of N phases, i.e. of N regions with energy bearing boundaries that may differ in their physical states. The different physical states can represent either different structures, compositions or orientations of the crystal lattice. To model multiphase systems, we introduce a vector-valued continuous order parameter $\boldsymbol{\phi}(\vec{x},t) = (\phi_1(\vec{x},t),\ldots,\phi_N(\vec{x},t))$ where each component $\phi_\alpha(\vec{x},t)$ of the vector describes the state of phase α and depends on a three-dimensional spatial coordinate $\vec{x}$ and on the time t. The formulation of the phase-field model for multiple order parameters is based on a Ginzburg-Landau energy density functional of the form

$$\mathcal{F}(\boldsymbol{\phi}) = \int_\Omega \Big(\varepsilon a(\boldsymbol{\phi},\nabla\boldsymbol{\phi}) + \frac{1}{\varepsilon} w(\boldsymbol{\phi}) + f(\boldsymbol{\phi})\Big)\, dx, \tag{1}$$

where Ω is the domain of consideration and ε defines the thickness of the diffuse interface in which the order parameters $\phi_\alpha(\vec{x},t)$ smoothly vary between two different physical states $\phi_\alpha(\vec{x},t)=1$ and $\phi_\alpha(\vec{x},t)=0$. As described in Eq. (6) of [8], the dynamical equations for the evolution of ϕ_α (the phase-field equations) are derived from the Ginzburg-Landau functional $\mathcal{F}(\boldsymbol{\phi})$ as variational derivatives with respect to the order parameters ϕ_α. In the following, we give examples for functional expressions of the three types of energy density contributions. The gradient energy density $a(\boldsymbol{\phi},\nabla\boldsymbol{\phi})$ can be formulated in terms of a generalized gradient vector $q_{\alpha\beta} = \phi_\alpha\nabla\phi_\beta - \phi_\beta\nabla\phi_\alpha$ by

$$a(\boldsymbol{\phi},\nabla\boldsymbol{\phi}) = \sum_{\alpha<\beta} \gamma_{\alpha\beta}|\phi_\alpha\nabla\phi_\beta - \phi_\beta\nabla\phi_\alpha|^2.$$

For simplicity, we assume the surface energy density $\gamma_{\alpha\beta}$ of the α/β boundary to be isotropic. The gradient vector $q_{\alpha\beta}$ is oriented in normal direction to the interface. Anisotropy of the surface energy can be introduced into the model by letting $\gamma_{\alpha\beta}$ depend on $q_{\alpha\beta}$ (see [8] for examples of functional expressions). The potential part $w(\boldsymbol{\phi})$ of the energy density functional is assumed to be a multi-obstacle type potential with higher order terms

$$w(\boldsymbol{\phi}) = \frac{16}{\pi^2}\sum_{\alpha<\beta}\gamma_{\alpha\beta}\phi_\alpha\phi_\beta + \sum_{\alpha<\beta<\delta}\gamma_{\alpha\beta\delta}\phi_\alpha\phi_\beta\phi_\delta. \tag{2}$$

The higher order terms $\sim \phi_\alpha\phi_\beta\phi_\gamma$ avoid the effect of ghost phase occurances at interfaces between two physical states. Further, we define free energy densities for the bulk states by

$$f(\boldsymbol{\phi}) = \sum_{\alpha=1}^{N} m_\alpha h(\phi_\alpha),$$

where $m_\alpha, \alpha = 1,\dots,N$ are constant factors related to the forces driving the phase transition. The function $h(\phi_\alpha)$ interpolates the energy densities between the bulk phases. We choose e.g. $h(\phi_\alpha) = \phi_\alpha$, $h(\phi_\alpha) = \phi_\alpha^2(3-2\phi_\alpha)$ or a higher order polynomial in ϕ_α.

In the following, the phase-field formalism is extended to situations in which a subset of order parameters has preserved volume. Without loss of generality, we assume the first $A \leq N$ physical states $\phi_\alpha, \alpha = 1,\dots,A$ to be subject of volume constraints. The states $\phi_\alpha, \alpha = A+1,\dots,N$ remain to be non-conserved order parameters and hence may undergo phase transitions or grain coarsening processes. To derive the model, we first introduce by rhs_α a short notation of the phase-field equations (Eq. (6) in [8])

$$\tau\varepsilon\partial_t\phi_\alpha = \underbrace{\varepsilon\left(\nabla\cdot a_{,\nabla\phi_\alpha}(\boldsymbol{\phi},\nabla\boldsymbol{\phi}) - a_{,\phi_\alpha}(\boldsymbol{\phi},\nabla\boldsymbol{\phi})\right) - \frac{1}{\varepsilon}w_{,\phi_\alpha}(\boldsymbol{\phi}) - f_{,\phi_\alpha}(\boldsymbol{\phi})}_{\mathrm{rhs}_\alpha} - \lambda, \qquad \alpha = 1,\dots,N \tag{3}$$

The parameter τ is a constant isotropic kinetic coefficient that may depend, in a general anisotropic system, on the orientation of the interface. The notation $a_{,\nabla\phi_\alpha}(\boldsymbol{\phi},\nabla\boldsymbol{\phi})$, $a_{,\phi_\alpha}(\boldsymbol{\phi},\nabla\boldsymbol{\phi})$, $w_{,\phi_\alpha}$ and $f_{,\phi_\alpha}(\boldsymbol{\phi})$ is used to indicate the partial derivatives of the functions $a(\boldsymbol{\phi},\nabla\boldsymbol{\phi})$, $w(\boldsymbol{\phi})$ and $f(\boldsymbol{\phi})$ with respect to $\partial\phi_\alpha$ and $\partial(\nabla\phi_\alpha)$. The time derivative $\partial\phi_\alpha(\vec{x},t)/\partial t$ is indicated by $\partial_t\phi_\alpha$ and $\nabla\cdot(\quad)$ denotes the the divergence of a vector field $a_{,\nabla\phi_\alpha}(\boldsymbol{\phi},\nabla\boldsymbol{\phi})$. The Lagrange multiplier λ is defined such that the constraint $\sum_{\alpha=1}^{N}\phi_\alpha(\vec{x},t) = 1$ is ensured. To establish volume conservation of individual ordering states $\phi_\alpha, \alpha = 1,\dots,A$, we propose an additional bulk energy density contribution $g(\boldsymbol{\phi})$ to the functional $\mathcal{F}(\boldsymbol{\phi})$ in Eq. (1) of the form

$$g(\boldsymbol{\phi}) = \sum_{\alpha=1}^{N}\chi_\alpha h(\phi_\alpha)$$

with $\chi_\alpha \neq 0$ for $\alpha = 1,\dots,A$ and $\chi_\alpha = 0$ for $\alpha = A+1,\dots,N$. By an appropriate choice of the parameters χ_α, the new function $g(\boldsymbol{\phi})$ is constructed in such a way that temporal changes in volume fraction of the conserved states are redistributed at the local interfaces. The phase-field equations with preserved volume can be rewritten as

$$\tau\varepsilon\partial_t\phi_\alpha = \mathrm{rhs}_\alpha - \lambda - g_{,\phi_\alpha}(\boldsymbol{\phi}) - \Lambda, \qquad \alpha = 1,\dots,N. \tag{4}$$

The derivative $g_{,\phi_\alpha}(\boldsymbol{\phi})$ of the redistribution energy density with respect to the order parameter ϕ_α

$$g_{,\phi_\alpha}(\boldsymbol{\phi}) = \chi_\alpha h_{,\phi_\alpha}(\phi_\alpha) \tag{5}$$

defines an anti-force term, precisely counterbalancing the change in volume fraction of the order parameter ϕ_α. The new redistribution force is accompanied by the occurance of an additional Lagrange multiplier Λ given by

$$\Lambda = -\frac{1}{N}\sum_{\alpha=1}^{N}\chi_\alpha h_{,\phi_\alpha}(\phi_\alpha). \tag{6}$$

For an ordering state being a conserved quantity, the integral of the respected order parameter ϕ_α over the entire volume Ω is a constant V_α. This constant is identical with the initial volume V_α^0 of the corresponding state

$$\int_\Omega \phi_\alpha dx = V_\alpha = \mathrm{const.}\Big(= \int_\Omega \phi_\alpha^0 dx = V_\alpha^0\Big). \tag{7}$$

The time derivative of the constant volume V_α vanishes

$$\int_\Omega \partial_t\phi_\alpha\, dx = \int_\Omega \frac{1}{\tau\varepsilon}\Big(\mathrm{rhs}_\alpha - \lambda - g_{,\phi_\alpha}(\boldsymbol{\phi}) - \Lambda\Big)\, dx = 0.$$

Using Eq. (4) we obtain a set of conditions that allow to determine the parameters χ_α ensuring volume conservation

$$\chi_\alpha = \begin{cases} \frac{1}{H_\alpha}\left(R_\alpha + \frac{1}{N-A}\sum_{\beta=1}^{A}R_\beta\right) & \text{for} \quad 1 \leq A < N \quad \text{and} \quad \alpha = 1,\dots,A \\ \frac{R_\alpha}{H_\alpha} & \text{for} \quad A = N \quad \text{and} \quad \alpha = 1,\dots,A. \end{cases} \tag{8}$$

In Eq. (8) we used the abbreviations

$$R_\alpha = \int_\Omega \Big(\mathrm{rhs}_\alpha - \lambda\Big)\, dx \qquad \text{and} \qquad H_\alpha = \int_\Omega h_{,\phi_\alpha}(\phi_\alpha)\, dx. \tag{9}$$

A finite difference method on a uniform rectangular mesh with an explicit time marching scheme is used to numerically solve the set of phase-field equations (Eq. (3)). We denote the time iteration by n with $n = 0, \dots, Nt$ and the space coordinates by i, j, k with $i = 0, \dots, Nx$, $j = 0, \dots, Ny$ and $k = 0, \dots, Nz$. The discrete time evolution of the order parameter ϕ_α reads

$$\widetilde{(\phi_\alpha)}^{n+1}_{i,j,k} = (\phi_\alpha)^n_{i,j,k} + \frac{\Delta t}{\tau\varepsilon}\Big((\mathrm{rhs}_\alpha)^n_{i,j,k} - \lambda^n_{i,j,k}\Big), \tag{10}$$

where Δt is an appropriate time step ensuring the stability of the explicit method. For the spatial derivatives in $(\mathrm{rhs}_\alpha)^n_{i,j,k}$, we apply forward and backward differences for the divergence of the flux $\nabla^l \cdot a_{,\nabla\phi_\alpha}(\boldsymbol{\phi}, \nabla^r\boldsymbol{\phi})$ and centered differences for the term $a_{,\phi_\alpha}(\boldsymbol{\phi}, \nabla^c\boldsymbol{\phi})$. We use the wide tilde $\widetilde{\phi_\alpha}$ notation to indicate an intermediate state of the order parameter ϕ_α before the volume change is redistributed by the execution of a suitable anti-forcing term. By substituting a sum over all grid points for the integral formulation in Eq. (7), the initial volume V^0_α and the volume V^n_α of the physical state ϕ_α at time n in the discrete computational domain Ω can be written as

$$V^0_\alpha = (\Delta x)^3 \sum_{i,j,k} (\phi_\alpha)^0_{i,j,k} \qquad \text{and} \qquad V^n_\alpha = (\Delta x)^3 \sum_{i,j,k} (\phi_\alpha)^n_{i,j,k}$$

From Eq. (10), the local change of the physical state ϕ_α at a grid point (i, j, k) from time n to $n + 1$ follows to be

$$\Big(\widetilde{(\phi_\alpha)}^{n+1}_{i,j,k} - (\phi_\alpha)^n_{i,j,k}\Big) = \frac{\Delta t}{\tau\varepsilon}\Big(\underbrace{(\mathrm{rhs}_\alpha)^n_{i,j,k} - \lambda^n_{i,j,k}}_{(R_\alpha)^{n+1}_{i,j,k}}\Big) \tag{11}$$

Volume preservation is achieved numerically by computing the anti-force $g_{,\phi_\alpha}(\boldsymbol{\phi})$ in Eq. (5) and the corresponding Lagrange multiplier Λ in Eq. (6) in a discrete form and as a function of the intermediate states $\widetilde{\phi_\alpha}$

$$g_{,\phi_\alpha}(\widetilde{\boldsymbol{\phi}})^{n+1}_{i,j,k} = \chi^{n+1}_\alpha\, h_{,\phi_\alpha}(\widetilde{(\phi_\alpha)}^{n+1}_{i,j,k}) \qquad \text{and} \qquad \Lambda^{n+1}_{i,j,k} = -\frac{1}{N}\sum_{\beta=1}^{N} \chi^{n+1}_\beta h_{,\phi_\beta}(\widetilde{(\phi_\beta)}^{n+1}_{i,j,k}). \tag{12}$$

Combining Eq. (9) and Eq. (11) gives

$$R^{n+1}_\alpha = (\Delta x)^3 \sum_{i,j,k} (R_\alpha)^{n+1}_{i,j,k} = \frac{\tau\varepsilon(\Delta x)^3}{\Delta t} \sum_{i,j,k} \Big(\widetilde{(\phi_\alpha)}^{n+1}_{i,j,k} - (\phi_\alpha)^n_{i,j,k}\Big) \quad \text{and} \quad H^{n+1}_\alpha = (\Delta x)^3 \sum_{i,j,k} h_{,\phi_\alpha}(\widetilde{(\phi_\alpha)}^{n+1}_{i,j,k}).$$

By inserting these relation into Eq. (8), the values of the counterbalance force χ^{n+1}_α can be computed. The time update of the order parameter $(\phi_\alpha)^{n+1}_{i,j,k}$ at time $n + 1$ ensuring volume preservation of the respective physical state is finalized by adding the redistribution force and the associated Lagrange multiplier in Eq. (12) with appropriate parameters $\frac{\Delta t}{\tau\varepsilon}\chi^{n+1}_\alpha$ to the intermediate state $\widetilde{(\phi_\alpha)}^{n+1}_{i,j,k}$, i.e.

$$(\phi_\alpha)^{n+1}_{i,j,k} = \widetilde{(\phi_\alpha)}^{n+1}_{i,j,k} - \frac{\Delta t}{\tau\varepsilon}\chi^{n+1}_\alpha\, h_{,\phi_\alpha}(\widetilde{(\phi_\alpha)}^{n+1}_{i,j,k}) - \frac{\Delta t}{\tau\varepsilon}\Lambda^{n+1}_{i,j,k}.$$

Since the initial volume of the physical state is preserved, i.e. $V^n_\alpha = V^0_\alpha$, we can exploit the simplification of Eq. (13)

$$R^{n+1}_\alpha = \sum_{i,j,k} \Big(\widetilde{(\phi_\alpha)}^{n+1}_{i,j,k} - (\phi_\alpha)^n_{i,j,k}\Big) = \sum_{i,j,k} \widetilde{(\phi_\alpha)}^{n+1}_{i,j,k} - \sum_{i,j,k} (\phi_\alpha)^n_{i,j,k} = \sum_{i,j,k} \widetilde{(\phi_\alpha)}^{n+1}_{i,j,k} - V^0_\alpha$$

in our numerical scheme.

To demonstrate the capability of the volume preserved multi-phase-field method, we study a bubble formation process as a minimum energy surface problem. An incompressibility of the bubble interior is assumed. In Fig. 1 a), a quadruple bubble ensemble was initially placed as four adjacent cubes of different phase-field parameters embedded in a matrix phase. In Fig. 1 b), a different initial setting with four adjacent spheroidal bubbles of identical volume,

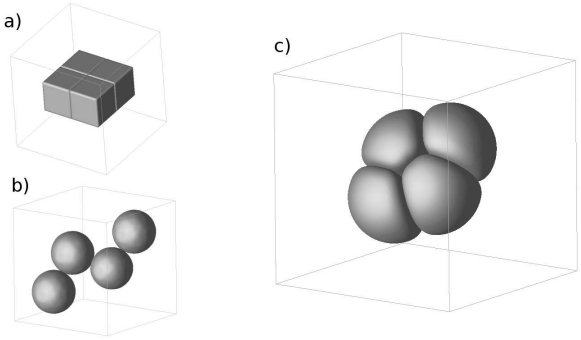

FIG. 1: a) and b) Two initial configurations of four bubbles in a matrix phase and c) final quadruple bubble configuration. For the simulations, a box of $75 \times 75 \times 75$ grid points was used with a regular grid spacing of $\Delta x = \Delta y = \Delta z = 0.02$ and a time constant of $\Delta t = 3.0e - 5$. The parameter of the higher order terms in Eq. (2) was set $\gamma_{\alpha\beta\delta} = 6.0$ and the surface energies of the boundaries are $\gamma_{\alpha\beta} = 1.0$.

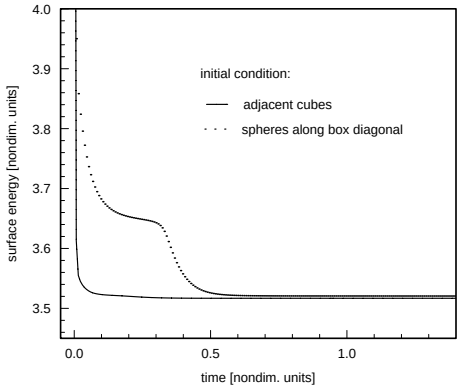

FIG. 2: Plot of the surface energy evolution for the two bubble configurations.

aligned in a zig-zag manner along the space diagonal of the box, was used. In both cases, the standard quadruple bubble in Fig. 1 c) forms which is the result of the initial configuration of Fig. 1 b). The result of the corresponding temporal evolution of the surface energy computed from the phase-field data according to Eq. (1) is illustrated in Fig. 2. The plateau in the dotted curve is due to the intermediate formation of a primary triple bubble cluster with a fourth adjacent neighbour.

Using 250 phase-field variables, we investigated grain coarsening in the presence of inert particle inclusions. The inert particles were represented by phase-field variables with constrained volumes. The 2D computational domain in Fig. 3 a) was randomly filled by a Voronoi partitioning algorithm. In Fig. 3 b), a snapshot of the grain boundaries after 16000 time steps is displayed showing a situation in which 13 % of the grains (marked in grey) have preserved volumes. If the volume of all phase fields is preserved, the system behaves as a polyhedral foam (Fig.3 c).

As a further application of the phase-field model with volume constraints, we study stable growth morphologies of double crystals, subject to a variable volume ratio $R = V_B/V_A$ of the two crystals A and B. In [6], the authors point out three mophology types in which bicrystals are formed in nature: Stacking faults breaking the translational symmetry of a crystal along a lattice direction, merohedral twins as in pyrite and the occurence of impurities along the interface. We choose anisotropies leading to square Wulff shapes for each of the two crystals (in 2D) and name the ratio between the internal crystalline boundary energy and the outer boundary energy by λ. Under this assumption, it has been proven in [6] that three different types of double crystals exist depending on the value of λ and R (see inset of Fig. 4): A rectangular bicrystal with continuous internal boundary (type I), a square crystal in contact with a rectangular one (type II) and a square-shaped bicrystal (type III). The geometric dimensions for each double crystal can be computed by minimizing the energy per unit length being a function of the dimension parameters x and y. By equating the surface energies of two double crystal types, the three theoretical curves shown as solid lines in the morphology diagram in Fig. 4 can be derived. The morphology diagram was scanned by systematic phase-field

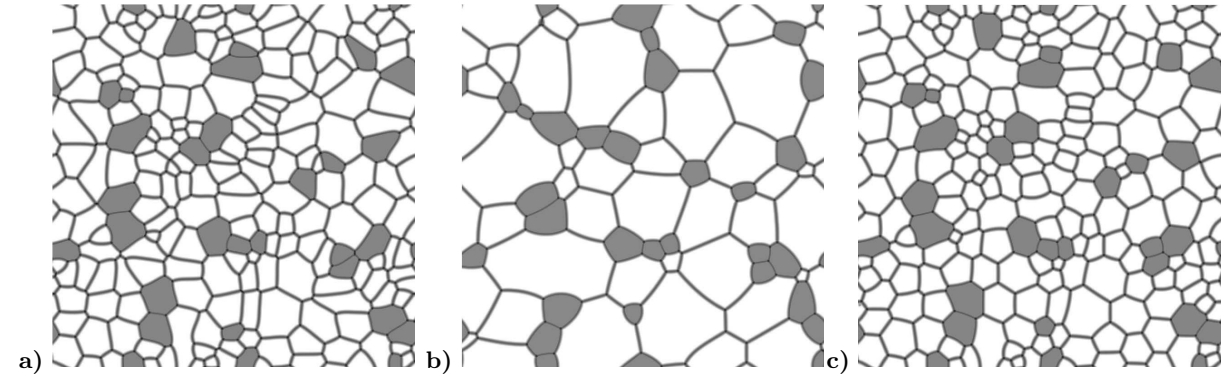

FIG. 3: a) Initial Voronoi distribution for multi-grain structures. The simulation results after 16000 time steps for b) a structure with 13 % of the grains with preserved volumes (marked in grey) is compared with a foam-like structure in c) with 100 % volume preservation. The parameters for the computations were 400×400 grid points, $\Delta x = \Delta y = \Delta z = 1.0$, $\Delta t = 0.8$, $\varepsilon = 3.0$, $\gamma_{\alpha\beta} = 0.25$ for all grain boundaries and $\gamma_{\alpha\beta\delta} = 3.0$.

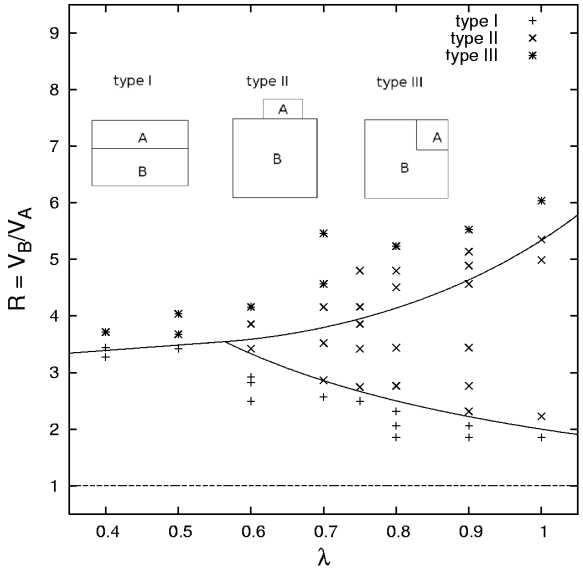

FIG. 4: Morphology diagram of double crystal configurations with theoretical coexistance curves of different crystal types (solid lines). The final morphologies of phase-field simulations are indicated as symbols referring to the different types (see inset). The computational parameters were 200×200 grid points, $\Delta t = 2.0e-5$, $\gamma_{\alpha\beta} = 1.0$ for the outer boundary of both crystals and $\lambda \in [0.4, 1]$ for the double crystal interface.

simulations of the microstructure evolution for different volume ratios R and different energy ratios λ. To perform the computations, the initial volume and shape of the crystal B was fixed whereas the volume of crystal A was changed to vary the volume ratio R. The initial setting was always a type II double crystal. To realize a facetted habit, a crystalline surface energy density of the form

$$a(\phi, \nabla\phi) = \sum_{\alpha<\beta} \gamma_{\alpha\beta} \Big(\max_{1\le k\le 4} \{ (\phi_\alpha \nabla\phi_\beta - \phi_\beta \nabla\phi_\alpha) \cdot \vec{\eta}_k \} \Big)^2$$

was used, where $\eta_k, k = 1, \ldots, 4$ denote four unit edge vectors of a square Wulff form. The edge vectors were chosen in diagonal direction of the coordinate system leading to the development of horizontal and vertical phase boundaries in the simulation box. In Fig. 4, the simulation results for discrete values of R and λ are plotted as symbols referring to the respective double crystal type. Starting with a homogeneous disperse distribution of the two crystal phases, the theoretical predictions of the morphology transitions are resolved well. Extended simulation studies in the region of the theoretical lines have shown a dependence of the final structure type on the intial condition. A detailled discussion

of the best choice of initial simulation configuration and an extension to a 3D morphology selection of double crystals is given in [11].

In conclusion, we have introduced a novel phase-field model that allows to treat pattern formations and microstructure evolutions in multiphase systems in which a subset of phases obeys volume constraints. Bubble clusters develop into an equilibrium configuration of minimal surface energy and the computational analysis of double crystal structures is consistent with theoretical predictions. The application to foam structures demonstrates the ability of the method to consider grain growth in the presence of phases with preserved volume fractions. It is expected that the presented phase-field model opens a broad range of new applications such as i.e. the study of inert particles in phase transformation processes, the inclusion of partial melts or bubbles in textures and the role of nucleation sides.

[1] B. Evans, J. Renner, G. Hirth, A few remarks on the kinetics of static grain growth in rocks, Intern. J. Earth Sc. 90 (2001), 88–103.

[2] J. Renner, B. Evans, G. Hirth, Grain growth and inclusion formation in partially molten carbonate rocks, Contr. Min. Petr. 142 (2002), 501–514.

[3] A. Elmoutaouakkil, L. Salvo, E. Maire, G. Peix, 2D and 3D Characterization of metal foams using X-ray tomography, Adv. Eng. Mat. 4 (2002), 803

[4] F. Graner, Y. Jiang, E. Janiaud, C. Flament, Equilibrium states and ground state of two-dimensional fluid foams, Phys. Rev. E 63 (2000), 011402-1–13.

[5] C. Carter, A. Roosen, J. Cahn, J.E. Taylor, Shape evolution by diffusion and surface attachment limited kinetics on completely faceted surfaces, Acta Metal. Mater. 43 (1995), 4309–4323.

[6] B. Wecht, M. Barber, J. Tice, Double crystals, Acta Cryst. A 56 (2000), 92–95.

[7] H. Garcke, B. Nestler, B. Stoth, A multi phase field concept: numerical simulations of moving phase boundaries and multiple junctions, SIAM J. Appl. Math. 60 (1999), 295–315.

[8] B. Nestler, H. Garcke, B. Stinner, Multicomponent alloy solidification: phase-field modeling and simulations, Phys. Rev. E 71 (2005), 041609-1–4.

[9] B. Stinner, Surface energies in multi-phase systems with diffuse phase boundaries, Free Boundary Problems, Intern. Ser. Numer. Math. 154, Birkhäuser (2007), 413–423.

[10] H. Garcke, B. Stoth, B. Nestler, Anisotropy in multi-phase systems: a phase field approach, Interf. Free Bound. 1 (1999), 175–198.

[11] Subject to a comprehensive study in a forthcoming paper.

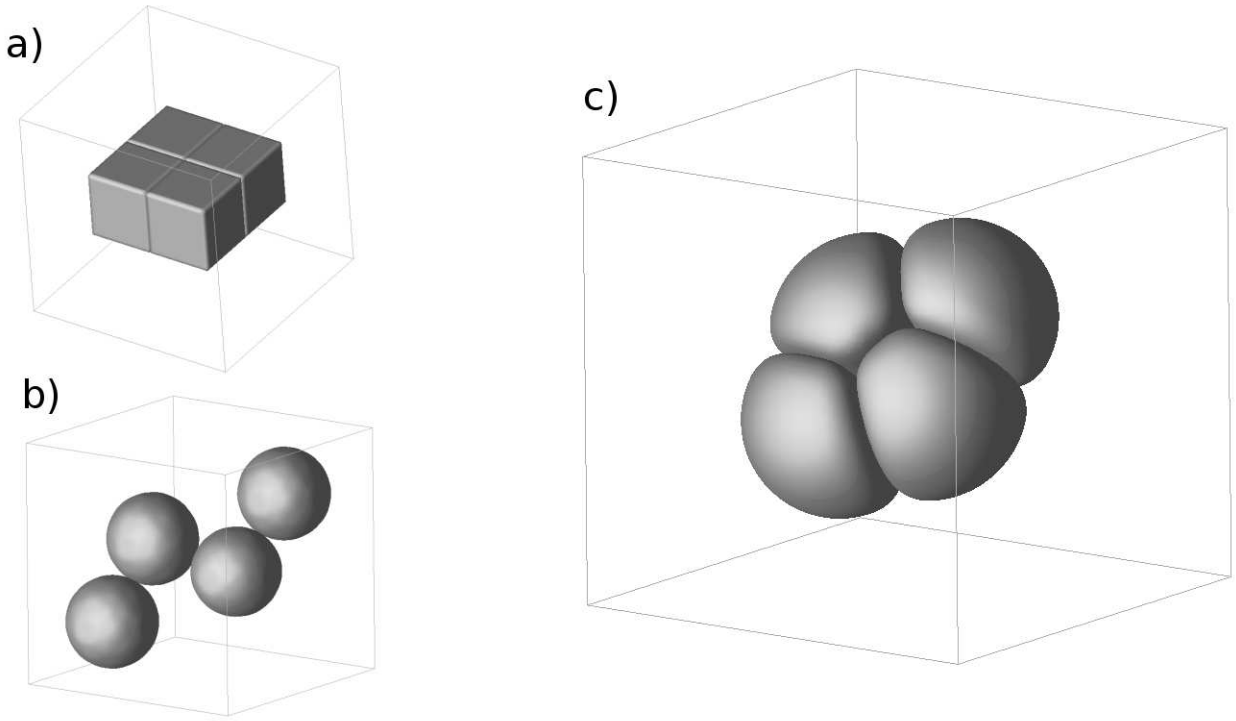

Figure 1

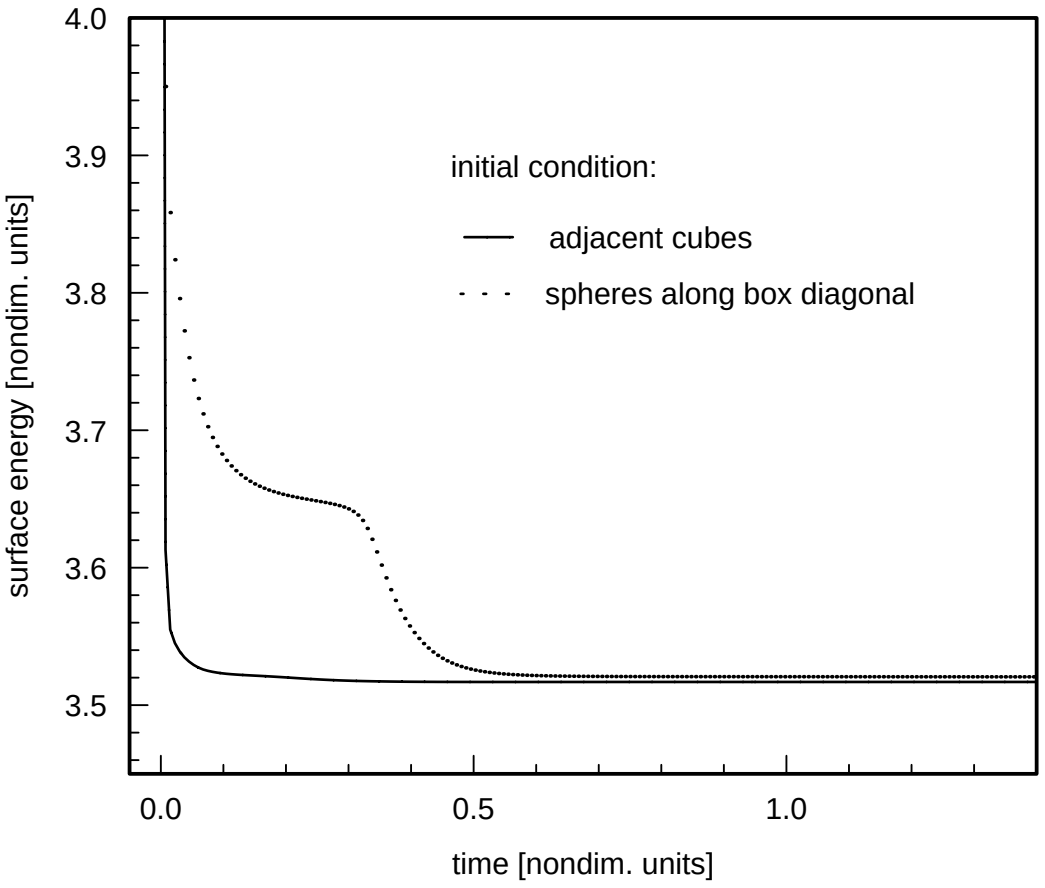
4.0
3.9
3.8
3.7
3.6
3.5
surface energy [nondim. units]
initial condition:
adjacent cubes
spheres along box diagonal
0.0
0.5
1.0
time [nondim. units]

Figure 2

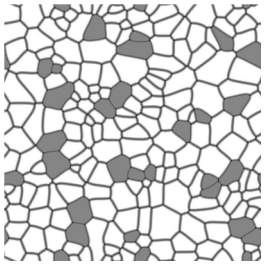

Figure 3a

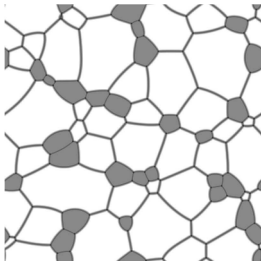

Figure 3b

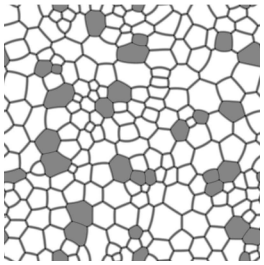

Figure 3c

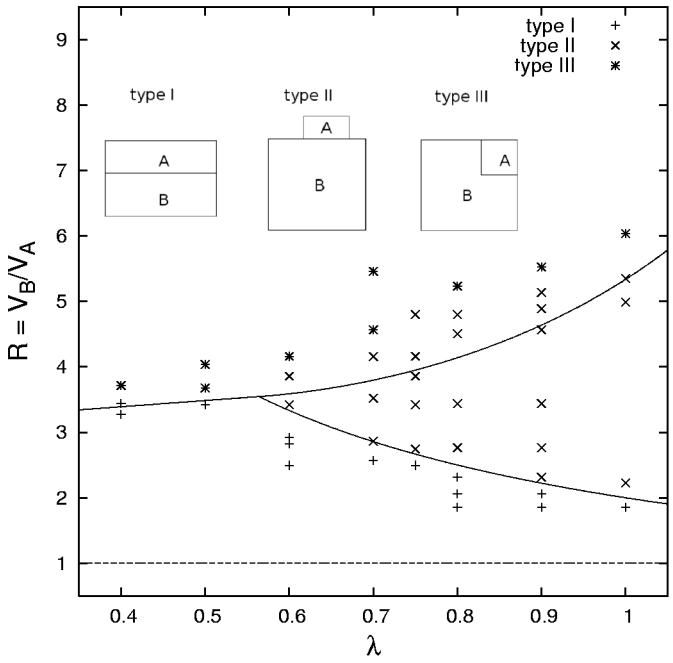
type I
type II
type III
type I
type II
type III
A
B
A
B
A
B
R = V_B/V_A
λ
9
8
7
6
5
4
3
2
1
0.4
0.5
0.6
0.7
0.8
0.9
1

Figure 4